



## Surface, thermal and hemocompatible properties of novel single stage electrospun nanocomposites comprising polyurethane blended with bio oil<sup>TM</sup>

MANIKANDAN AYYAR<sup>1</sup>, MOHAN PRASATH MANI<sup>2</sup>, SARAVANA KUMAR JAGANATHAN<sup>3,4,5</sup>, RAJASEKAR RATHINASAMY<sup>6</sup>, AHMAD ZAHRAN KHUDZARI<sup>5</sup> and NAVANEETHA PANDIYARAJ KRISHNASAMY<sup>7</sup>

<sup>1</sup>Department of Chemistry, Bharath University, Chennai 600073, Tamil Nadu, India

<sup>2</sup>Faculty of Biosciences and Medical Engineering, Universiti Teknologi Malaysia, Skudai 81300, Johor Bahru, Malaysia

<sup>3</sup>Department for Management of Science and Technology Development, Ton Duc Thang University, Ho Chi Minh City, Vietnam

<sup>4</sup>Faculty of Applied Sciences, Ton Duc Thang University, Ho Chi Minh City, Vietnam

<sup>5</sup>IJNUTM Cardiovascular Engineering Centre, Department of Clinical Sciences, Faculty of Biosciences and Medical Engineering, Universiti Teknologi Malaysia, Skudai 81300, Johor Bahru, Malaysia

<sup>6</sup>Department of Mechanical Engineering, Kongu Engineering college, Perunduari 638052, Tamil Nadu, India

<sup>7</sup>Department of Physics, Sri Sakthi Institute of Engineering and Technology, Coimbatore 641062, Tamil Nadu, India

*Manuscript received on March 27, 2017; accepted for publication on June 12, 2017*

### ABSTRACT

In this work, the physicochemical and blood compatibility properties of prepared PU/Bio oil nanocomposites were investigated. Scanning electron microscope (SEM) studies revealed the reduction of mean fiber diameter ( $709 \pm 211$  nm) compared to the pristine PU ( $969 \text{ nm} \pm 217$  nm). Fourier transform infrared spectroscopy (FTIR) analysis exposed the characteristic peaks of pristine PU. Composite peak intensities were decreased insinuating the interaction of the bio oil<sup>TM</sup> with the PU. Contact angle analysis portrayed the hydrophobic nature of the fabricated patch compared to pristine PU. Thermal gravimetric analysis (TGA) depicted the better thermal stability of the novel nanocomposite patch and its different thermal behavior in contrast with the pristine PU. Atomic force microscopy (AFM) analysis revealed the increase in the surface roughness of the composite patch. Activated partial thromboplastin time (APTT) and prothrombin time (PT) signified the novel nanocomposite patch ability in reducing the thrombogenicity and promoting the anticoagulant nature. Finally the hemolytic percentage of the fabricated composite was in the acceptable range revealing its safety and compatibility with the red blood cells. To reinstate, the fabricated patch renders promising physicochemical and blood compatible nature making it a new putative candidate for wound healing application.

**Key words:** Polyurethane, Bio oil<sup>TM</sup>, Nanocomposite, atomic force microscopy, wound healing.

### INTRODUCTION

Cooking and other common activities in restaurants where people works in hot environment, there

is a high probability for burn injuries which is inevitable due to fatigue and improper handling. A burn injury is also one of the common household injuries for kids (Forastieri 1997). Apart from these, fire accidents and also war field activities are some of the events causing burns (Reason 2016). The

Correspondence to: Saravana Kumar Jaganathan  
E-mail: [saravana@tdt.edu.vn](mailto:saravana@tdt.edu.vn)

biological process involved in the healing of burn is rather complex and may result the skin cells to die. Burn injury patients require immediate attention and proper treatment depending upon the stages of burn wound, otherwise leading to life-threatening events to simple scars depending upon the degree of burn wound (Ghieh et al. 2015).

The most common treatment for burn wounds involves applying dressing material on top of the wounds. The ideal dressing material should be capable of providing moist environment for stimulating re-epithelization, inhibit the microbial invasion and retard the fluid loss from the body (Hong et al. 2009). Blood is the common connective tissue which comes in contact with the dressing material used to assist the wound healing. So, first and foremost, any dressing material utilized for wound healing should be compatible with blood. The influence of fabricated dressing material on the activation of blood clots through intrinsic and extrinsic pathways was signified using the APTT and PT assay respectively. Further, haemolysis assay is a simple and important blood compatibility test as it is found to be an indicator of cytotoxicity nature of the fabricated material to the red blood cells. Whenever, RBCs comes in contact with water, they are subjected to complete lysis by releasing hemoglobin and other biomolecules. However, the similar lysis phenomenon is also observed during contact with foreign substances due to excessive osmotic stress exerted from the incompatible material surface (Yuan et al. 2013). So, there is a continuous search for such dressings with improved properties which facilitate the wound healing without causing damage to blood. With the advent of nanotechnology, researchers employ electrospun nanofibers because of its high surface to volume ratio and its close resemblance with the extracellular matrix as an excellent scaffold for the regeneration of epithelial skin cells (Unnithan et al. 2012).

Electrospinning is a cost effective and versatile method which involves applying high voltage to

polymer melts which is drawn into nanofibers at the collector end. Even though it was invented 100 years ago, the utilization of electrospinning for biomedical application has been flourished only in last few decades (Unnithan et al. 2012, Chen et al. 2008). Polyurethane is one of the commonly used polymers for making wound dressings in the forms of foams, membranes and films etc. Fabrication of nanofibers from PU is easy which makes them commonly used electrospun polymer for medical application. This polymer is already employed in several clinical applications and its biodegradable nature excellently matches the formation of new extracellular matrix and also tissue regeneration process (Guo and Ma 2014, Grzesiak et al. 2015). In this research, tecoflex EG80A which is poly-ether based medical grade polyurethane was used to fabricate the nanofibers.

Bio oil™ is the commercially available oil to assist wound healing and reduce scar formation. It contains vitamins and plant extracts in oil-base which helps to retain the potency of the active constituents (Avaialble at <https://www.bio-oil.com/en-us/>). In this work, a novel bio nanocomposite utilizing PU and bio oil™ will be fabricated using single step electrospinning process to assist the burn wound healing. The aim of this work will be fabrication and physico-chemical characterization of the developed nanocomposite. Further, blood compatibility assays will be performed to assess the compatibility of the composite along with the pure polyurethane nanofibers with the surrounding tissues.

## MATERIALS AND METHODS

Tecoflex EG-80A medical-grade thermoplastic polyurethane (PU) was purchased from LubriZol, USA. N, N-dimethylformamide (DMF) were supplied by Merck Millipore, Germany. The commercially available bio oil™ was obtained locally. Phosphate buffered saline (PBS, Biotech Grade) and sodium chloride physiological saline

(0.9% w/v) was supplied by Sigma-Aldrich, Malaysia. The reagents used in APTT and PT assay such as rabbit brain activated cephaloplastin, calcium chloride (0.025 M), and thromboplastin (Factor III) were supplied by Diagnostic Enterprises, India.

#### PREPARATION OF NANOCOMPOSITE

To prepare the polymer melts, 480 mg of PU beads were dissolved in 6 ml of DMF by magnetic stirring for 24 h at room temperature to obtain a homogenous solution of concentration 8% (w/v). 400 µl of bio oil™ was mixed with 4.6 ml of DMF to make 8% v/v solution and stirred for 1 h minimum to obtain a homogenous solution. Finally, the PU/bio oil™ nanocomposite was prepared by slowly adding bio oil™ solutions in PU at a ratio of 8:2 under rigorous stirring for 60 min.

#### FABRICATION OF PU AND NANOCOMPOSITE DRESSING

Pure PU nanofiber and PU/bio oil™ nanocomposite was electrospun according to the following method. Prepared solutions of PU and composite was aspirated inside the plastic syringe of 10 ml with 18-G stainless steel needle and attached to the syringe pump (SP20, NFiber). NFiber high voltage unit was used to supply the voltage required for electrospinning. Nanofibers were collected on a static drum collector covered with aluminium foil. After several trials, the PU was successfully electrospun at a flow rate of 1.0 ml/hr with an applied voltage of 10 kV. The addition of bio oil™ reduced the viscosity of the nanocomposite solution. Hence, the flow rate and voltage were changed to 0.50 ml/hr and 7 kV, respectively, to obtain a steady stream of the polymer solution. Collector distance was constantly maintained at 16 cm for both samples. The deposited nanofibrous mesh was carefully detached from the collector and dried at room temperature for 24 h.

#### PHYSICOCHEMICAL CHARACTERIZATION

##### SCANNING ELECTRON MICROSCOPY (SEM) MICROGRAPHS

The fiber diameter and the morphology of the electrospun PU and the bio oil™ nanocomposite were studied using a Hitachi Tabletop SEM unit (TM3000). The samples were gold coated before obtaining the photomicrographs. The diameter size distribution in the fabricated membranes was determined using ImageJ (National Institutes of Health, Bethesda, MD) software by measuring at least 30 individual fibers randomly. The mean and standard deviation of the diameter distribution was obtained from ImageJ software.

##### ATTENUATED TOTAL REFLECTANCE FOURIER TRANSFORM INFRARED SPECTROSCOPY (ATR-FTIR) ANALYSIS

The chemical composition of the electrospun PU and the bio oil™ nanocomposite were studied using the ATR-FTIR unit. For recording the IR spectra of PU and bio oil™ nanocomposite, a small amount of the sample was placed on the sensor surface and the spectra were captured. Meanwhile, the IR spectrum of bio oil™ was obtained by placing a drop of the sensor surface. The spectra of each sample were recorded over the range of 600-4000 cm<sup>-1</sup> at 32 scans per minute and averaged at the resolution of 4 cm<sup>-1</sup>. Zinc Selenium (ZnSe) was used as an ATR crystal which was coupled with the NICOLET IS5 spectrometer. The spectra were baseline corrected and normalized using Spekwin32 software to identify the characteristic peaks and differences.

##### CONTACT ANGLE MEASUREMENT

The wettability of electrospun PU and the bio oil™ nanocomposite was calculated using the VCA Optima contact angle measurement unit. Sample of size 1 X 5 cm<sup>2</sup> were cut from the mesh for measuring the contact angle. After fitting the syringe loaded with the water, a droplet of size 2

$\mu\text{L}$  was formed at the tip and it was carefully placed on the test membrane. A static image of the liquid deposition within few seconds was obtained using a high-resolution video camera. The contact angle of samples was measured by three different trials and the manual contact angle was obtained through computer integrated software.

#### THERMOGRAVIMETRIC ANALYSIS

The thermal stability of electrospun PU and the bio oil<sup>TM</sup> nanocomposite was studied using the PerkinElmer TGA 4000 unit. Sample mass of 3 mg were placed in an aluminium pan and the experiment was carried out under a dry nitrogen atmosphere in the temperature range 30 - 1500°C at an ascending rate of 10°C/min. The remaining weight of the sample was recorded at each temperature point and the values were exported in an excel sheet. Then, the TGA curve and the corresponding derivative weight loss curve (DTG) were drawn using OriginPro 8.5 software.

#### ATOMIC FORCE MICROSCOPY

Atomic force microscopy was used to measure the sample surface roughness (Ra) and to obtain 3D image of the sample surface JPKSPM data processing software was used. For this, sample of size 1 X 1 cm<sup>2</sup> were cut from the mesh placed on the AFM equipment (Nanowizard, JPK instruments) and scanned for measuring the surface roughness. All samples were scanned at room temperature in normal atmosphere. The scanning size was 20  $\mu\text{m}$   $\times$  20  $\mu\text{m}$  and the images are captured in the medium mode with 256 x 256 pixels.

### HEMOCOMPATIBILITY ASSESSMENT OF THE DRESSING MATERIAL

#### ETHICAL STATEMENT AND COLLECTION OF BLOOD SAMPLES

All the experimental procedures involved in the handling of blood were approved by Faculty

of Biosciences and Medical Engineering, Universiti Teknologi Malaysia with ref no UTM.J.45.01/25.10/3Jld.2(3). The blood was collected from healthy adults who were educated about the risk and benefits of the blood donation. The blood was collected via venipuncture after getting a signature in the consent form. The collected blood was anticoagulated with acid-citrate-dextrose (ACD) (56 mM sodium citrate, 65 mM citric acid, 104 mM dextrose) at a ratio of 9:1 (blood/citrate). Finally, citrated blood was centrifuged at 3000 rpm for 15 min to extract platelet poor plasma (PPP).

#### ACTIVATED PARTIAL THROMBOPLASTIN TIME (APTT) ASSAY

PU and the PU/bio oil<sup>TM</sup> dressings were cut into square samples of dimension 0.5 x 0.5 cm<sup>2</sup>. For each dressings assay was performed in triplicate, so three square samples of each type were introduced into 96 well plates and gently washed with deionized water. The samples were incubated in PBS at 37°C for 30 min before starting the assay. First, 50  $\mu\text{l}$  of obtained PPP was placed on the sample and incubated for 1 min at 37°C and then 50  $\mu\text{l}$  of rabbit brain cephaloplastin reagent was added and incubated for 3 min at 37°C. Finally, the reaction mixture was activated by adding 50  $\mu\text{l}$  of CaCl<sub>2</sub> and gently stirred with a sterile steel needle. The time taken for the formation of the white fibrous clot was noted using a chronometer.

#### PROTHROMBIN TIME (PT) ASSAY

Fabricated membrane was cut into square samples as described in the previous subdivision and this test was also performed in triplicate. Samples were washed with deionized water and incubated in PBS for 30 min at 37°C. To begin the assay, 50  $\mu\text{l}$  of PPP was added to the sample at 37°C for 1 min, followed by addition of 50  $\mu\text{l}$  of NaCl-thromboplastin reagent (Factor III) and gently mixed with a sterile steel needle until clot formation. The time taken for the clot formation was noted as PT.

#### HAEMOLYSIS ASSAY

Thermoset Scientific Multiskan™ FC (Waltham, MA, USA) was used to investigate the effect of fabricated membranes with red blood cells. For this both PU and the fabricated samples (1 x 1 cm<sup>2</sup>) were soaked in physiological saline (0.9%w/v) at 37°C for 30 min. Next, they were exposed with a mixture of aliquots of citrated blood and diluted saline (4:5) for 1 h at 37°C. For constituting positive and negative control, the whole blood was mixed with distilled water (4:5) (complete haemolysis) and also with physiological saline solution respectively. The exposed samples were retrieved and the mixtures were centrifuged at 3000 rpm for 15 min. The supernatant was aspirated and the absorbance of each sample was recorded at 542 nm which directly represents red blood cell (RBC) damage. The percentage of hemolysis or hemolytic index was calculated using the formula, Hemolysis ratio (HR) = (TS-NC)/(PC-NC) x 100 (Balaji et al. 2016) where TS, NC, and PC are measured absorbance values of the test sample, negative control and positive control at 542 nm, respectively.

#### STATISTICAL ANALYSIS

All experiments were conducted thrice independently. Unpaired t-test was done to determine statistical significance. The results obtained from all experiments are expressed as mean ± SD. In case of qualitative experiments, a representative of three images is shown.

#### RESULTS AND DISCUSSION

Scanning electron microscope results indicated the random morphology of the fibers as shown in Fig. 1a and 1b. Image J analysis of the SEM Fig. 1 showed that polymer PU has a mean diameter and standard deviation of 969 nm ± 217 nm. Similarly for the PU/bio oil™ composite mesh the fiber diameter was found to be 709 ± 211 nm as indicated in Fig. 1c

and 1d respectively. The fiber diameter was found to reduce within the nanocomposite compared with the pure PU nanofibers. This diameter reduction may be attributed to the conductivity change of the polymer solution when mixed with the bio oil™. As the bio oil™ is found to possess several constituents like vitamins and plant extracts, it may result in the increased conductivity, leading to the stretching and elongation of fiber resulting in the diameter reduction. Similar observation was reported recently when honey and papaya was added to the PU resulting in diameter reduction (Balaji et al. 2016). Further, Kumbar et al. 2008 worked on the optimization of fiber diameter of scaffolds for skin graft using PLGA as a model polymer. They found that fiber diameter of 600- 1200 nm was able to support the highest proliferation of fibroblast cells compared with other diametric ranges. They also found that collagen III expression was also following the same trend in this range of diameter. Our scaffolds diameter are within the range of these reported values and indicated its promising quality in supporting the proliferation of fibroblast cells which is an essential process in wound remodelling. Kwon and Matsuda 2005 utilized electrospinning technique for fabricating biodegradable scaffold based on poly (L-lactide-co-caprolactone) (PLCL) nanofibers blended with collagen and heparin. In this research, the developed PLCL composites scaffolds showed reduced fiber diameter with the improved fiber density and mechanical strength. It was also observed that the composite fabrics scaffold with small diameter rendered enhanced adhesion and proliferation of umbilical vein endothelial cells (HUVEC's) on its surface. Hence PU/bio oil™ composite with reduced diameter may be expected to favour the significant proliferation of cells on the surface of the scaffold for new tissue growth.

FTIR analysis depicts the functional groups present in the samples. The FTIR of the PU, PU/bio oil™ composite mesh and bio oil™ expressed



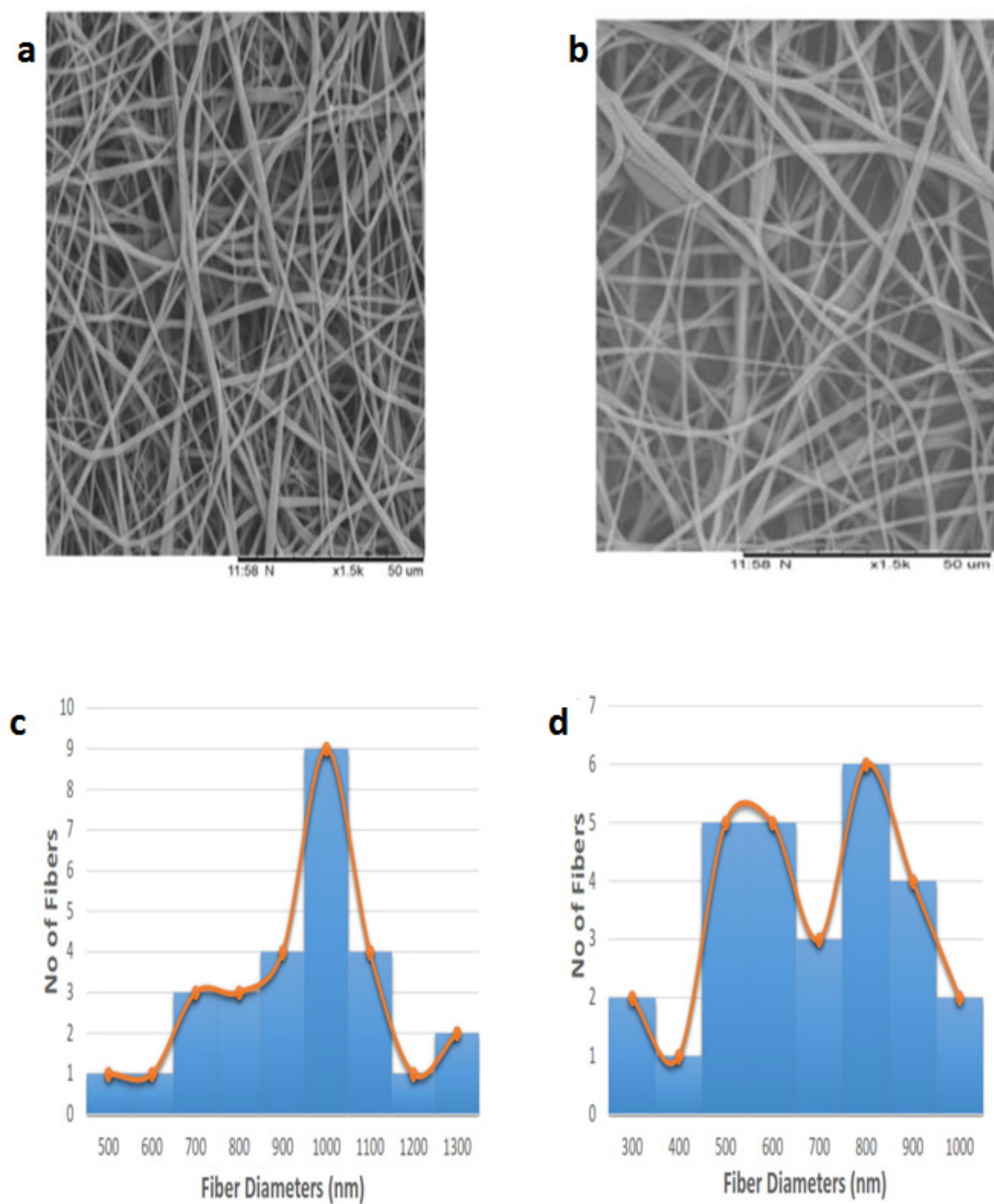


**Figure 1** - SEM images of a) Pure Polyurethane b) Polyurethane/bio oil™ composites c) Fiber diameter of PU d) Fiber diameter of PU/bio oil™ composites.

difference in the FTIR spectra as shown in Fig. 2. The pure PU spectra indicated key peaks which were reported already. The peak exhibited at  $3323\text{ cm}^{-1}$  represented the characteristic NH stretching of an aliphatic primary amine and its vibration were seen at the peak  $1597\text{ cm}^{-1}$  and  $1531\text{ cm}^{-1}$  respectively. Peaks at  $2939\text{ cm}^{-1}$  and  $2854\text{ cm}^{-1}$  represents the CH stretching and other vibrations of CH can be inferred at the peaks  $1413\text{ cm}^{-1}$ . Further, a twin peak noted at  $1730\text{ cm}^{-1}$  and  $1703\text{ cm}^{-1}$  indicate the C=O stretching of carboxylic groups whilst the sharp peaks formed at  $1221\text{ cm}^{-1}$ ,  $1104\text{ cm}^{-1}$  and  $770\text{ cm}^{-1}$  specify the C-O stretching corresponding to alcohol groups. Similar observations were reported by Jia et al. 2014 and Kim et al. 2009. FT-IR spectrum of bio oil™ showed a sharp peak between  $2922\text{ cm}^{-1}$  to  $2852\text{ cm}^{-1}$  indicate C-H stretch and its vibration was seen at  $1463\text{ cm}^{-1}$  respectively. The peak at  $1737\text{ cm}^{-1}$  corresponds to the vibrations of C=O stretching. The spectrum of the fabricated nanocomposite showed no additional bands but the characteristic peaks of PU were found to be decreased. This may be attributed due to the formation of hydrogen bond (Unnithan et al. 2012). Further, the presence of bio oil™ molecules in the PU was identified by slight shifting of CH peak in pure PU from  $2939\text{ cm}^{-1}$  to

$2926\text{ cm}^{-1}$  in PU/bio oil™ composites which clearly indicates that interaction between the PU has bio oil™ constituents (Tijing et al. 2012).

Contact angle measurements of pristine PU and the PU/bio oil™ composite meshes fabricated by electrospinning were done and shown in Table I. The mean contact angle of the PU is  $86^\circ$  whereas, the nanocomposite mesh displayed the contact angle of  $115^\circ$  as shown in Fig. 3a and 3b. It indicates that there is a tendency for the nanocomposite mesh to turn hydrophobic as the water contact angle exceeded  $90^\circ$ . Ceylan 2009 and Cui et al. 2008 had suggested that the reduction in fiber diameter generally increases the water contact angle. Our results are also in favour of this findings as we could observe the reduction in the fiber diameter of the nanocomposite mesh.

Thermal analysis of the composite patches along with the pure polyurethane was done as indicated in Fig. 4. The onset temperature of the pure PU was found to be  $273^\circ\text{C}$ , whereas the composite PU with bio oil™ exhibited a higher temperature of onset  $284^\circ\text{C}$  as noted in Fig. 4a and 4b. The thermal degradation behaviour pattern of the PU and PU/bio oil™ are different with each other because the incorporated constituents of bio oil™ affected the thermal property. To further state,

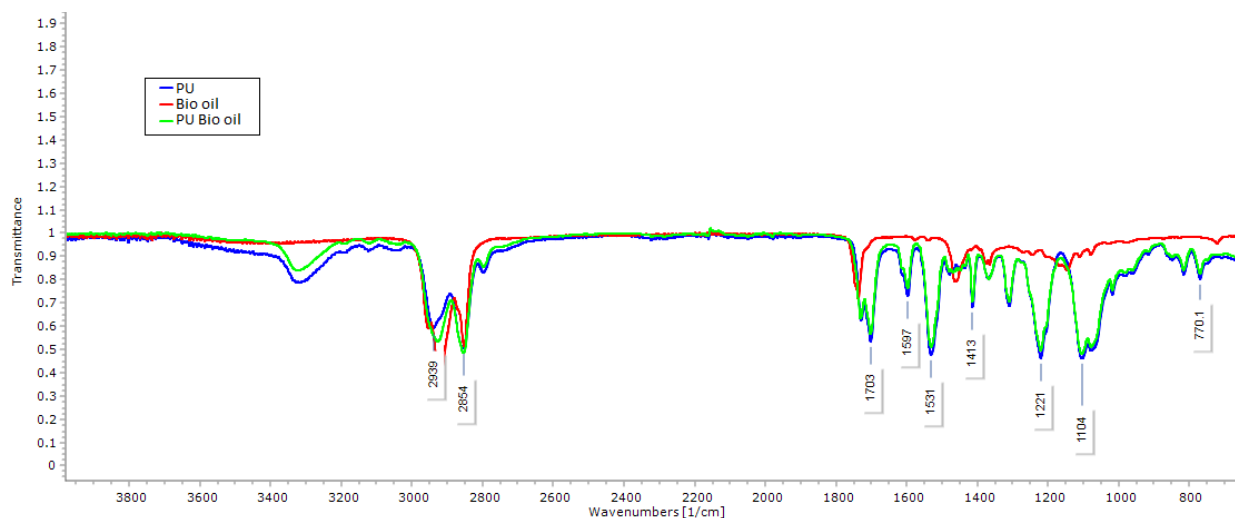


**Figure 2** - FTIR analysis of pure PU, bio oil™ and PU/bio oil™ composites.

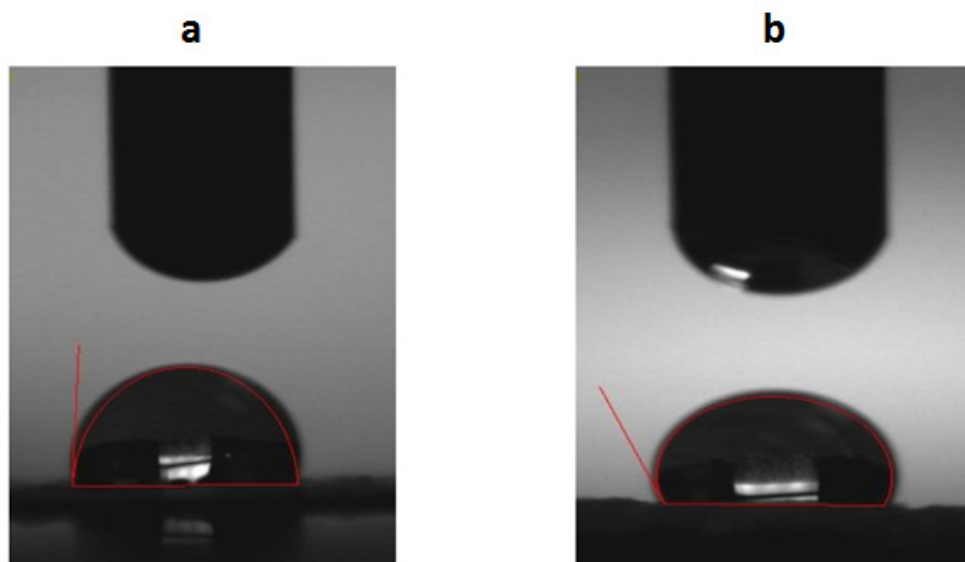


**Figure 3** - Contact angle images of **a)** Pure Polyurethane and **b)** PU/bio oil™ composites.

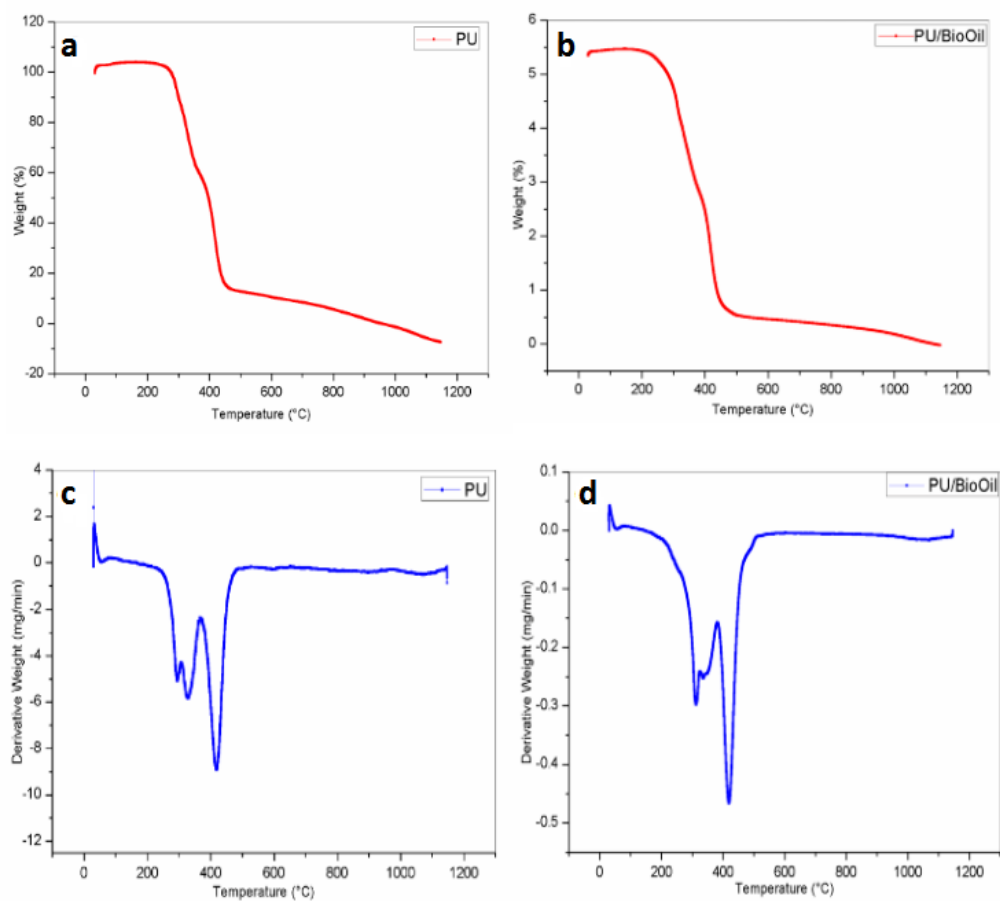


**Figure 4** - TGA analysis of **a)** Pure Polyurethane **b)** Polyurethane/bio oil™ composites **c)** Weight residue percentage of Pure PU and **d)** Weight residue percentage of PU/bio oil™ composites.



the added constituent's active groups enhanced the thermal stability of pristine PU nanofibers. Finally, the percentage residual weight of the pristine and the composite material at 950°C was found to be 0.08 and 4.50% as noted in Fig. 4c and 4d. This concludes that developed nanocomposite have better thermal stability due to the addition of bio oil™. Baştürk et al. 2016 reported the thermal stability of the polyurethane composites incorporated with barium metaborate and observed that the addition of barium metaborate into polymer matrix improved the thermal behaviour of polyurethane. Similar observations were reflected in these experimental results.

Atomic force microscopic analysis of fabricated composite and pure PU patch was performed to compute the surface roughness as shown in Fig. 5a and 5b. The surface roughness of the pristine PU and the composite patch were found to be 723 nm and 1326 nm (Ra) respectively. The addition of bio oil™ to the pristine PU increased the surface roughness and similar observation was reported in the recent work by Moradi et al. 2015. They found that addition of graphene in to PVDF membrane enhanced the surface roughness and its hydrophobic nature. In a similar coincidence, the fabricated composite patch showed increasing hydrophobic nature as reported in the contact angle section.

Blood compatibility of the mesh was done to understand its compatibility with the surrounding blood. The fabricated composite and the pristine PU was assessed for their APTT and PT times which are the indicators of intrinsic and extrinsic pathways associated with blood clotting respectively. In the APTT assay, the PU nanofiber membrane exhibited a mean clotting time of  $157.3 \pm 5.55$  s while the fabricated PU/bio oil™ composite exhibited delay in the clotting with the mean value of  $191.7 \pm 1.34$  s as indicated in Fig. 6. This observation illustrates the antithrombogenicity of the fabricated patch. There is a delay in the clotting time APTT insinuating that the nanocomposite surface is better than the pure

PU surface. This is vital because the fabricated material may not induct the intrinsic pathway faster compared to pure PU patch promoting the anticoagulant nature of the polyurethane composite. Similarly, the role of extrinsic and common pathways cannot be undermined in rendering the anticoagulant nature, hence, the PT time for the above-said nanocomposite and the pure PU patch was performed. PT assay revealed the clotting time of the PU/bio oil™ composite was prolonged until  $48.33 \pm 0.57$  s from the mean clotting time of  $38.3 \pm 1.15$  s as noted in PU (Fig. 6). Delay in the clotting times may be attributed to the enhanced surface properties. It has been reported that the smaller fiber diameter will be conducive for blood compatibility. In their work, they fabricated scaffolds of different diameter using two polymers namely degarapol and PLGA and they found scaffolds of smaller diameter irrespective of polymer nature displayed a delay in the coagulation cascade which is analogous to the observed findings (Vincent et al. 2012). Further, the presence of bio oil™ based constituents might also play a vital role in delaying the clotting time. Finally, the haemolytic percentage of the fabricated PU and composite was evaluated. The haemolytic percentage depicts the safety of the fabricated patch against red blood cells. Haemolytic percentage was computed by recording the absorbance of obtained supernatant after blood reacts with the composite patch at 542 nm. The absorbance value of PU was significantly higher than that of the PU/bio oil™ composite indicating lysis of erythrocytes by pristine PU. The hemolytic index of PU was found to be 2.733% whereas for bio-nanofibrous membrane it was only 0.95% as shown in Fig. 6. According to ASTM F756-00(2000) standard, hemolysis percentage above 5% was considered haemolytic and the percentage between 2 to 5% was classified as slightly haemolytic material. On the other hand, if the material has a hemolysis percentage below 2 it is considered to be a non-hemolytic material (Elahi

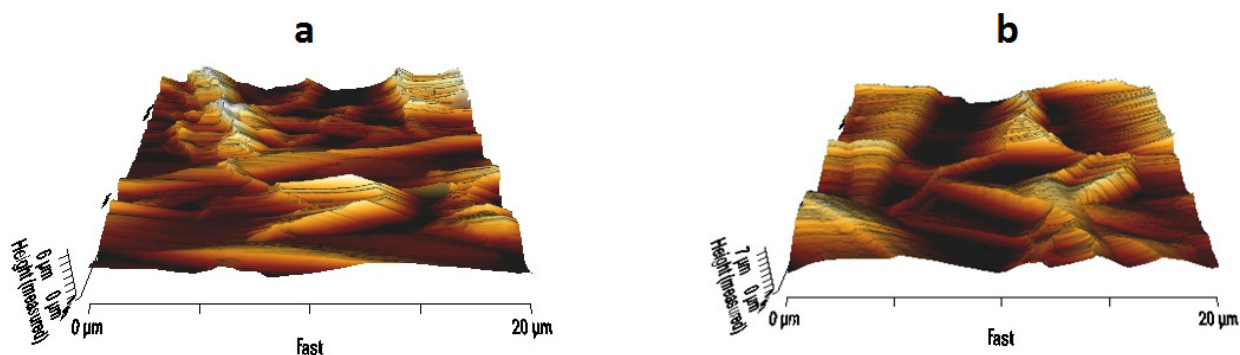
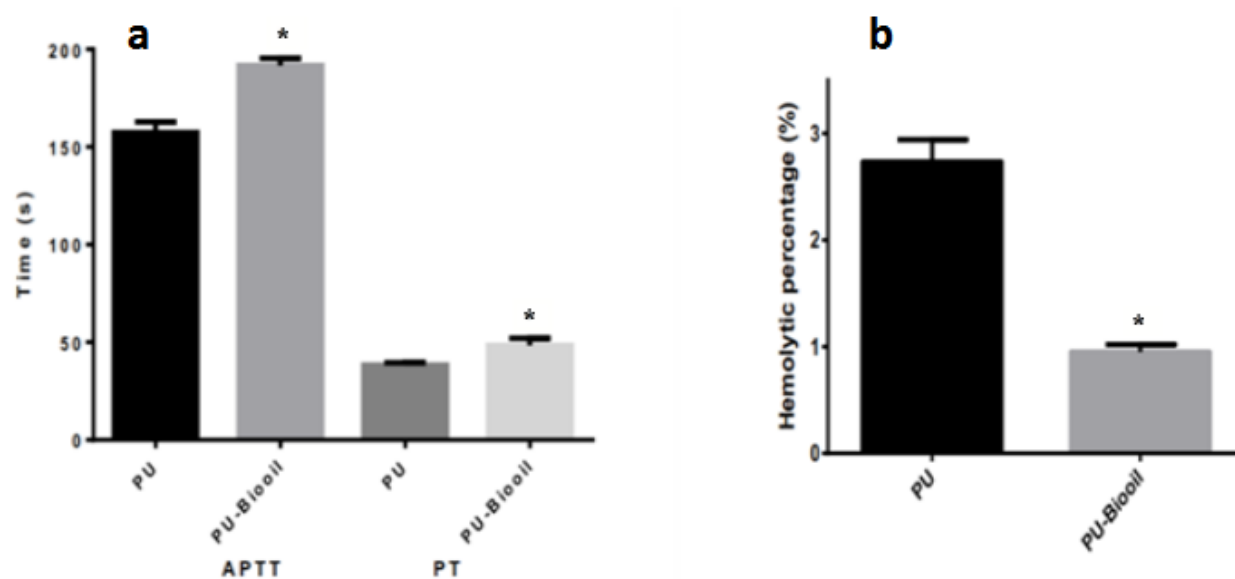


Figure 5 - AFM analysis of a) Pure Polyurethane b) PU/bio oil™ composites.



\*mean differences were significant compared with pure PU ( $p < 0.05$ ).

Figure 6 - a) APTT and PT assay of Pure Polyurethane and PU/bio oil™ composites and b) Hemolysis assay of PU and PU/bio oil™ composites.

et al. 2014). Since the fabricated patch haemolytic percentage was below 1% indicated its non-hemolytic behaviour. Recently, Balaji et al. 2015 investigated the blood compatibility of microwave assisted-metallocene polyethylene (mPE) coated with aloe vera for tissue engineering applications. It was reported that the surface modified mPE displayed enhanced blood compatibility owing to presence of active constituents present in the aloe vera. Since our fabricated nanocomposites showed enhanced blood compatibility and this might

favours tissue rehabilitation process for wound healing applications.

## CONCLUSIONS

In nutshell, the fabricated PU composite patch possessed smaller diameter compared to the pure PU. FTIR analysis indicated the interaction between the PU and bio oil™ as evident through hydrogen bonding and peak shifting. The hydrophobic nature of the composite was illustrated through

the increasing contact angle compared to pristine PU. Further, TGA analysis depicted the better thermal stability of the fabricated composite patch. In addition, AFM analysis depicted an increase in the surface roughness value insinuating the morphological changes in the composite patch. The fabricated PU/bio oil™ composite mesh expressed a significant delay in blood clotting indicated through their APTT and PT values. This in turn confirms the antithrombogenic nature of the composite patch in comparison with the pure PU patch. Finally, the haemolytic percentage came in support that the fabricated novel composite patch found to less haemolytic material. These results are in favour that the fabricated composite patch may serve as a putative material in the wound dressing. However further experiments like animal and cellular testing may further make the fabricated PU/bio oil™ composite patch as an important dressing agent promoting the wound healing.

#### ACKNOWLEDGMENTS

This work was supported by the Ministry of Higher Education Malaysia with the Grant no. Q.J130000.2545.17H00. The authors declare that they have no conflict of interest.

#### REFERENCES

- BALAJI A, JAGANATHAN SK, ISMAIL AF AND RATHINASAMY R. 2016. Fabrication and hemocompatibility assessment of novel polyurethane-based bio-nanofibrous dressing loaded with honey and carica papaya extract for the management of burn injuries. *Int J Nanomed* 11: 4339-4355.
- BALAJI A, JAGANATHAN SK, SUPRIYANTO E, MUHAMAD II AND KHUDZARI AZM. 2015. Microwave-assisted fibrous decoration of mPE surface utilizing Aloe vera extract for tissue engineering applications. *Int J Nanomedicine* 10: 5909-5923.
- BAŞTURK E, MADAKBAŞ S AND KAHRAMAN MV. 2016. Improved Thermal Stability and Wettability Behavior of Thermoplastic Polyurethane / Barium Metaborate Composites. *Mater Res* 19(2): 434-439.
- CEYLAN M. 2009. Superhydrophobic behavior of electrospun nanofibers with variable additives. Available at <http://hdl.handle.net/10057/2535>.
- CHEN JP, CHANG GY AND CHEN JK. 2008. Electrospun collagen/chitosan nanofibrous membrane as wound dressing. *Colloids Surf A: Physicochem Eng Asp* 313: 183-188.
- CUI W, LI X, ZHOU S AND WENG J. 2008. Degradation patterns and surface wettability of electrospun fibrous mats. *Polym Degrad Stability* 93(3):731-738.
- ELAHIMF, GUANG AND WANG L. 2014. Hemocompatibility of surface modified silk fibroin materials; a review. *Rev Adv Mater Sci* 38: 148-159.
- FORASTIERI V. 1997. Children at work: Health and Safety risks, 2nd edition., International Labour Organization.
- GHIEH F, JURJUS R, IBRAHIM A, GEAGEA AG, DAOUK H, BABA BEL, CHAMS S, MATAR M, ZEIN W AND JURJUS A. 2015. The Use of Stem Cells in Burn Wound Healing: A Review. *BioMed Res Int* 2015: 1-9.
- GRZESIAK J, MARYCZ K, SZAREK D, BEDNARZ P AND LASKA J. 2015. Polyurethane/poly(lactide)-based biomaterials combined with rat olfactory bulb-derived glial cells and adipose-derived mesenchymal stromal cells for neural regenerative medicine applications. *Mater Sci Eng C* 52: 163-170.
- GUO BL AND MA PX. 2014. Synthetic biodegradable functional polymers for tissue engineering: a brief review. *Sci China Chem* 57(4) : 490-500.
- HONG SI, CHOI WY, CHO SY, JUNG SH, SHIN BY AND PARK HJ. 2009. Mechanical properties and biodegradability of poly-3-caprolactone/soy protein isolate blends compatibilized by coconut oil. *Polym Degrad Stability* 94: 1876-1881.
- JIA L, PRABHAKARAN MP, QIN X AND RAMAKRISHNA S. 2014. Guiding the orientation of smooth muscle cells on random and aligned polyurethane/collagen nanofibers. *J Biomater Appl* 29: 364-377.
- KIM SE, HEO DN, LEE JB, KIM JR, PARK SH, JEON SH AND KWON IK. 2009. Electrospun gelatin/polyurethane blended nanofibers for wound healing. *Biomed Mater* 4: 044106.
- KUMBAR SG, NUKAVARAPU SP, JAMES R, NAIR LS AND LAURENCIN CT. 2008. Electrospun poly(lactic acid-co-glycolic acid) scaffolds for skin tissue engineering. *Biomater* 29(30): 4100-4107.
- KWON IK AND MATSUDA T. 2005. Co-Electrospun Nanofiber Fabrics of Poly(L-Lactide-Co-Epsilon-Caprolactone) With Type I Collagen or Heparin. *Biomacromol* 6(4): 2096-2105.
- MORADI R, JAVAD KS, MOJTABA SN AND KOOCHAKI MA. 2015. Preparation and Characterization of Polyvinylidene Fluoride/Graphene Superhydrophobic Fibrous Films. *Polym* 7(8): 1444-1463.

- REASON J. 2016. Managing the risks of organizational accidents, Taylor and Francis Group. ISBN 13: 978 1 84014 104 7: 1-243.
- TIJING LD, RUELO MTG, AMARJARGAL A, PANT HR, PARK CH, KIM DW AND KIM CS. 2012. Antibacterial and superhydrophilic electrospun polyurethane nanocomposite fibers containing tourmaline nanoparticles. *Chem Eng J* 197: 41-48.
- UNNITHAN AR, NASSER AMB, TIRUPATHI PICHIAH PB, GOPALSAMY G, NIRMALA R, CHAD YS, JUNGE CH, MOHAMED ELN AND KIM HY. 2012. Wound-dressing materials with antibacterial activity from electrospun polyurethane–dextran nanofiber mats containing ciprofloxacin HCl. *Carbohydr Polym* 90: 1786-1793.
- VINCENT M, THOMAS H, HEIKE H, VIOLA V AND DANIEL E. 2012. Influence of fiber diameter and surface roughness of electrospun vascular grafts on blood activation. *Acta Biomater* 8(12): 4349-4356.
- YUAN W, FENG Y, WANG H, YANG D, AN B, ZHANG W, KHAN M AND GUO J. 2013. Hemocompatible surface of electrospun nanofibrous scaffolds by ATRP modification. *Mater Sci Eng C* 33: 3644-3651.